FINAL YEAR PROJECT II

Synthesis and Characterization of Titania Photocatalyst Nano-particles of Controlled size and Shapes for waste water treatment

By

Khethiwe Judith Mkhatshwa
Supervisor
Dr Sujan Chowdhurry

Progress Report submitted in partial fulfillment of
the requirements for the Final Year Project
Bachelor of Engineering (Hons)
(Chemical Engineering)

July 2013

Universiti Teknologi PETRONAS
Bandar Seri Iskandar
31750 Tronoh
Perak Darul Ridzuan

ACKNOWLEDGEMENTS

First and foremost, I would like to thank God for giving me this opportunity to do this project and to study in UTP and also my family for their love and encouragement over this period of my time in Malaysia. This project would not have been there if the university didn’t create such an exposure for their students hence my gratitude extends to UTP for the opportunity to do the final year project especially the department of chemical engineering. My gratitude extends to my Supervisor Dr Sujan Chowdhurry who was there every step of the way in the project. His support, attention and advices really helped the advancement and completion of my project. My appreciation extends to the lab technicians for teaching me how to use the equipment’s and for always providing all the apparatus that I needed when I asked for them. Keep on with the dedication provided to me as I am certain other students will appreciate it too. I would like to express my appreciation to Mrs Susan who has assisted me in getting the project started by her training sessions and other provisions. My gratitude also extends to my lab mate Lee Yi tong for her assistance in making the project a success. Finally, I want to thank everyone who directly or indirectly contributed to the completion of this work because without you, I wouldn’t make it.

.

ABSTRACT

Titania nanotube was synthesized through the hydrothermal route and used for the degradation of azo dye (Sulfan blue) by means of photocatalysis process. The particle sizes, surface morphology, crystal structure were characterized by field emission scanning electron microscopy (FESEM), transmission electron microscopy (TEM), X-ray diffraction (XRD) and Brunauer-Emmett-Teller (BET). The length of the tubes were found to be 150-300nm from the FESEM and BET measured a surface area of 277.17 m^2/g, the adsorption model on the titanate nanotube and titania follows the type v Isotherm (multilayer) . The XRD surfaced a formation of anatase phased $TiO_{2.}$ The degradation of Sulfan blue dye was more favourable in alkaline solution, with an optimum (pH 14) while varying the dosage of the TiO_2 from (0.025-0.2) g revealed an increase in the rate of degradation, the optimum dosage was found to be 0.2 g. Furthermore, the titania nanotube degradation rate was higher compared to the commercial TiO_2 (p25) because of the larger surface area. The adsorption kinetics for the adsorption was done following the type 1 pseudo first order model, type 1 pseudo second order model among others for a comparison between commercial titania and titanate nanotube. The adsorption kinetics display that the degradation follows a type 1 Pseudo second order model.

TABLE OF CONTENTS

LIST OF FIGURES

LIST OF TABLES

CHAPTER 1

INTRODUCTION

1.1 Background of study

Dyestuff leaked into wastewater due to inefficiency is turning into a principal source of pollution. A projected 10-20% of dyes are discharged to the environment [1]. There are various processes that have been employed nowadays to treat the dyed waste water namely, Adsorption, Ion exchange, reverse Osmosis. However of this processes photo catalysis process is substantially the prominent process by far. Photo catalysis is a process in which light it absorbed by the photo catalyst and the electrons at the valence band will be excited to the conduction band [1-5].

Electron excites to the conduction band and it creates a hole in the valance band, thus forming hydroxyl radicals which have the capacity to degrade the organic material (dye pollutant) by forming less carcinogenic compound such as water and $CO_{2.}$ Titanium dioxide is used as the photocatalyst because it exhibits various appreciable characteristics hence it is widely used in photocatalysis; these impressive qualities encompass a high catalytic competence, affordability, low toxicity and its translucence to visible light. Titanium dioxide has 3 crystal structures namely (a) Anatase, (b) Rutile and (c) Brookite, Fig 1 illustrates these different crystal structures Anatase has the highest band gap energy compared to rutile and brookite hence it is widely used for synthesis of the hierarchical structures of $_{TiO2}$ (one dimensional, two dimensional and three dimensional). The degradation of any organic matter is much more rapid in anatase phase, the degradation reaction is affected by the crystalline state and the physical properties such as the particle size and higher surface area [6]. Therefore, in this study we synthesized the rich in anatase phase one dimensional TiO_2 with an impressive 80% anatase crystallinity using hydrothermal method.

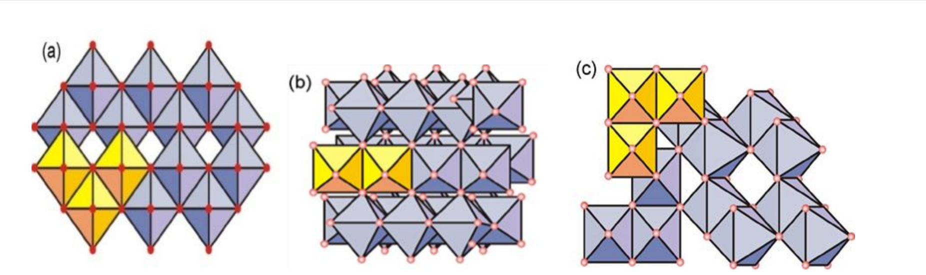

Figure 1: Titanium dioxide crystalline structures

Numerous studies have been done on the degradation of dye through photocatalysis [2, 4, 6-8]. The degradation process is affected by several factors which have been studied such as the pH effect, photocatalyst dosage, temperature and concentration of dye. pH plays an important role in the degradation process because it controls the acidic and base state of the solution moreover the degradation is also dependent on the dosage of the photocatalyst because it is also a driving force for the degradation [2-4, 6, 8-10].

In this study, one-dimensional titanate nanotubes were synthesized using hydrothermal method. The structural feature of the TiO_2 nanoparticles were determined with Scanning electron microscope (SEM), transmission electron microscope (TEM), electron energy loss spectroscopy (EELS), X-ray powder diffraction (XRD), Energy Dispersive X-ray Spectroscopy (EDX), Fourier Transform Infrared Spectroscopy (FTIR), Electron diffraction (ED), N_2 adsorption-desorption technique and UV-vis absorption spectroscopy.

The degradation kinetics is discussed only for the titanate nanotube and the commercial titania. Azo dye (Sulfan blue) degradation was done for commercial TiO_2 (p25) and synthesized titania nanotube for comparison under UV-light. The governing parameters used are the pH effect and TiO_2 dosage. The degradation data was fitted in specialized kinetic models to determine the best fit. The degradation of the titania nanotube and the titanium dioxide follows the same kinetic models due to their similarity in properties. The best fit is categorized by the coefficient given that is the R^2 value from the linear equation of the graph. The higher the R^2 value the closer will be the proposed experimental Q to the calculate [11].

In this study the models used for the adsorption is the type I pseudo-first-model, type 2 and 5 pseudo-second order models fitted based on the experimental data obtained from the degradation of Sulfan blue onto commercial titanium dioxide and the titanate nanotube.

Problem Statement

Dyes are a threat to the environment. Industries releasing dye in wastewater have to reduce the carcinogenic nature of the dyes because if released directly to the environment they will cause a lot of hazards hence the best way to release them without any harm is by reducing the colorization through the photo catalytic process. The degradation is usually done by TiO_2 (p25) however in this project it shall be done also with the synthesized titanate nanotube to compare the rate of degradation. The synthesis is done to improve the crystallinity of the TiO_2 in order to make the degradation of the dye pollutant favorable.

1.3 Objectives

The main objectives of this study are:

i) To synthesize the one dimensional (Titanate nanotube) structure through the hydrothermal route.
ii) To study the degradation of dye using TiO_2 (Powder and nanotube)

1.4 Scope of study

The scope of study based on the objectives can be simplified as follows:

i) Synthesize the titanate nanotubes structures of TiO_2 using the hydrothermal experimental method with solvent namely Sodium hydroxide (NaOH)
ii) Study the particle sizes and shapes (Sample characterization)
iii) Investigate the different adsorption parameters (*pH effect, TiO_2 dosage)*

CHAPTER 2

LITERATURE REVIEW

Titanium dioxide can be transformed in various structures ranging from rod, square and flower-like shapes moreover classified by their crystallinity as one dimensional, two dimensional and three dimensional structures. The synthesis of the square-like titanium structure can be done via the hydrothermal route [12]. The characterization of the samples is done by the transmission electron microscopy (TEM) and the XRD (X-ray diffraction) and SEM-Scanning Electron Microscope. The instruments used to study the surface morphology and to determine the amount of TiO_2 present in the sample [3,5, 13-19]. Sample characterization plays an important role because if there are impurities in the samples they will be shown in the sample characterization equipment. There are various articles that report on the synthesis of the (3D)/flower-like structure of titania through a similar method of the hydrothermal route [18] intended for the use as photocatalyst to degrade dye pollutants in waste water.

The method that seems to be cost effective is the adsorption of the dye through the natural ways which is by the use of Papaya leaf powder however it is not efficient than photocatalysis [7]. The parameters of adsorption that were studied in the majority of the articles were the pH effect and the photocatalyst dosage. The degradation of methylene blue dye revealed a high dependence in the pH of the solution, thus instigating the adsorbent to have expedient surface charge for the methylene blue adsorption [4, 7, 9]. These results can also be expected for the adsorption of Sulfan blue unto titanium dioxide surface.

The degradation of Sulfan blue dye through photocatalysis is dominantly dependent on the dosage and the pH effect by commercial titania (p25) [1]. The trend is also expected when studying the degradation of the dye with the one dimensional $TiO_{2.}$ Titanium dioxide can be promoted by impregnating activated carbon in order to improve its photocatalytic activity, a comparison was done between the commercial titania and the TiO_2 impregnated activated carbon to degrade indigo carmine dye. The degradation was optimised through dye concentration and catalyst amount [10].

The degradation of Methylene blue are optimised following the same aspects that is dye concentration and catalyst amount with an addition of pH effect, however new parameters are introduced such as effect of reaction temperature [4]. The customary kinetic models used to explain the solid/liquid equilibrium adsorption processes are the pseudo-first order and the pseudo-second-order model [7]. There are other various linear models which have been proposed for the solid/liquid adsorption processes which are the (type 1-type 5) Pseudo second order models [11]. The Adsorption Isotherms also play an important role in characterizing the type of adsorption that take place,that is monolayer or multilayer adsorption, Langmuir and freundlich respectively. Studies have been done on the degradation of Sulfan blue using the TiO_2 photocatalyst [1] however the kinetics were not presented.

The degradation kinetics of reactive dyes such as safira HEXL dye, an anionic azo dye can be conducted through the Langmuir-Hinshelwod model. The main parameters optimized in are the effect of pH,amount of photocatalyst, UV light intensity in a TiO_2 in a slurry reactor [8]. The kinetics of photocatalytic decomposition of methylene blue is also analyzed in the same procedure which is according to the Langmuir-Hinshelwood equation rate, the additional operating factors include the agitation speed, recirculation flow rate, initial dissolved oxygen concentration and reaction temperature [4]

CHAPTER 3
METHODOLOGY

This chapter covers the methodology used in conducting this project. The chapter presents the steps, approach, taken to synthesize the Titanate nanotube, characterization of the sample as well as application into waste water treatment. The Flow chart, list of materials and the equipment used are presented as well.

Table 1: Chemicals used for the experiment

Chemical Name	**Chemical Formula**	**Molecular Mass (g/mol)**	**Supplier**	**Purpose**
Titanium dioxide (p25)	TiO_2	79.87	Merck	TN synthesis
Sodium Hydroxide	NaOH	39.997	R&M chemicals	TN synthesis
Hydrochloric acid	HCL	36.46	Merck	Purification
Sulfan blue/ Patent blue	$C_{27}H_{31}N_2NaO_7S_2$	582.66	Sigma-Aldrich	Waste water
Perchloroethylene	Cl2C:CCl2	165.83	J.T. Baker	Waste water
Potassium hydroxide	KOH	56.12	Merck	TN synthesis
De-Ionized water	H_2O	18.01	--------	Solvent
Distilled water	H_2O	18.01	--------	Solvent

Table 2: Equipment used and tools used in the experiment

Equipment / tool	**Purpose**
Magnetic Stirrer	Stirring of chemicals
Drying oven	Synthesis of TN
Vacuum oven	Drying of TN
UV-Spectrophotometer	Rate of degradation
Field Emission Electron Microscope	Surface morphology and structure
TEM	Particle size and crystal structure
UV-Fabricated box	To degrade the dye pollutant

3.1 Flowchart

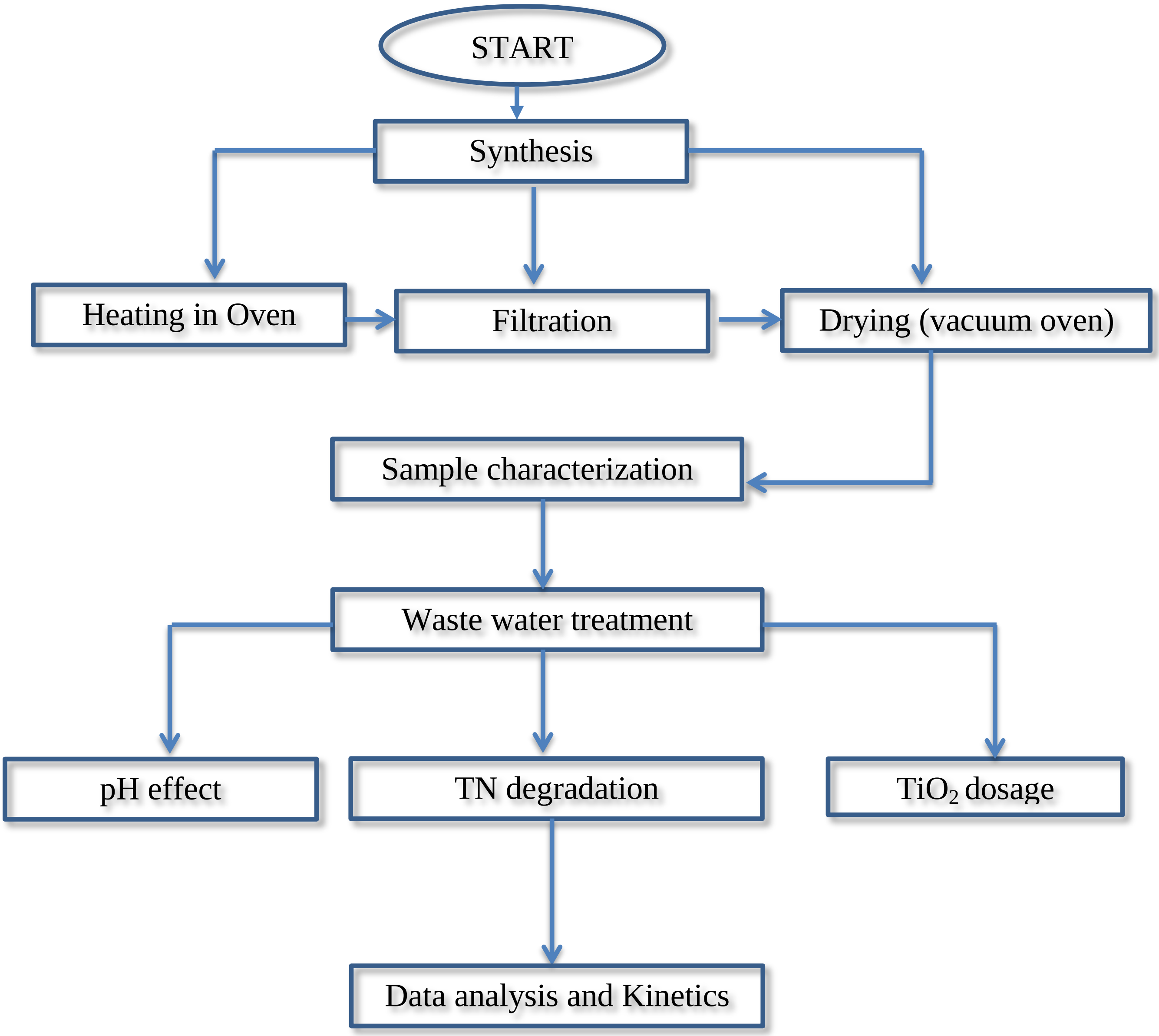

3.2 Methodology explained

Synthesis and characterization of TN (Titanate nanotube):

The one dimensional structure is synthesized by mixing 0.1 gram of titanium dioxide (p25) with 10mol/l of sodium hydroxide. The mixture is stirred briefly for 10min to ensure that the TiO_2 is dissolved in the solvent. The NaOH acts as a surfactant because it stretches the TiO_2 thus forming the rod. The sample is stirred and introduced in the 65ml Teflon-lined autoclave and introduced into a normal oven where it is heated at 150^oC for 48hours, the high temperature and the pull from the surfactant results in the formation of the one dimensional structure.

The sample from the oven is left to cool overnight to ambient temperature. After cooling it is filtered with 0.03M of HCl to remove impurities (purification). The purified sample is dried in a vacuum oven for 6 hrs to remove the moisture. The dried sample is crushed using a mortar to maintain fine particles. After the sample is prepared it is taken for characterization to study the surface morphology.

Waste water treatment (pH effect and TiO_2 dosage):

A solution of 0.06 g/L of Sulfan blue is prepared using de-ionized water. The pH of the solution is varied from (pH 4- pH 14) by adding droplets of Sodium hydroxide. A dose of 0.1 g of Commercial Titanium dioxide was mixed with the Sulfan blue solution and stirred in the UV box. The sample is then taken at different time intervals to monitor the degradation rate. The UV-visible equipment was used to determine the absorbance of the different samples.

An optimum pH is obtained from the UV-visible results which precedes the experiment to the TiO_2 dosage. The same procedure is used in the TiO_2 dosage experiment however the pH is kept constant. Only the Optimum pH obtained from the pH effect experiment is used in the dose effect. The concentration of the dye is also kept constant. The dose is varied from (0.05- 2 grams). The last part of the experiment is using the one dimensional structure (TN) that was synthesized via the hydrothermal route to degrade the dye. The conditions of the experiment are constant dye concentration and a dosage of 0.1 gram is used. A comparison between the TN and the commercial TiO_2 is done to determine the most efficient in degrading the dye.

CHAPTER 4

RESULTS AND DISCUSSION

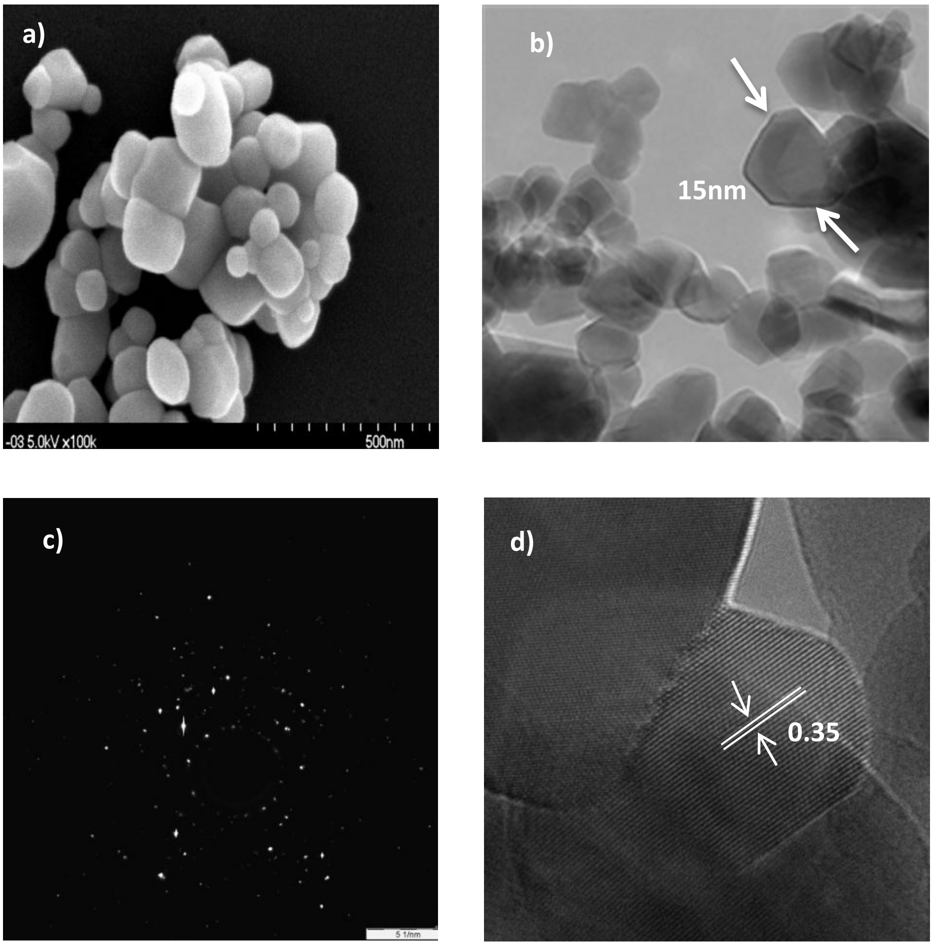

Figure 2: FESEM image (a) TEM (b) HRTEM image (d) and SAED image(c) for commercial TiO_2

The commercial titanium dioxide characterization results are illustrated in Fig 2. The surface morphology of the titania is shown in the FESEM and TEM presented by fig 1(a- b) to be circular-like nanoparticles with a size of 7-30 nm. The HRTEM image in Fig. 1d depicts the lattice fringe of 0.35nm represented by the [101] plane in the XRD data. The electron diffraction represented by Fig 1c shows that a single circular-like nanoparticle demonstrates an anatase planar.

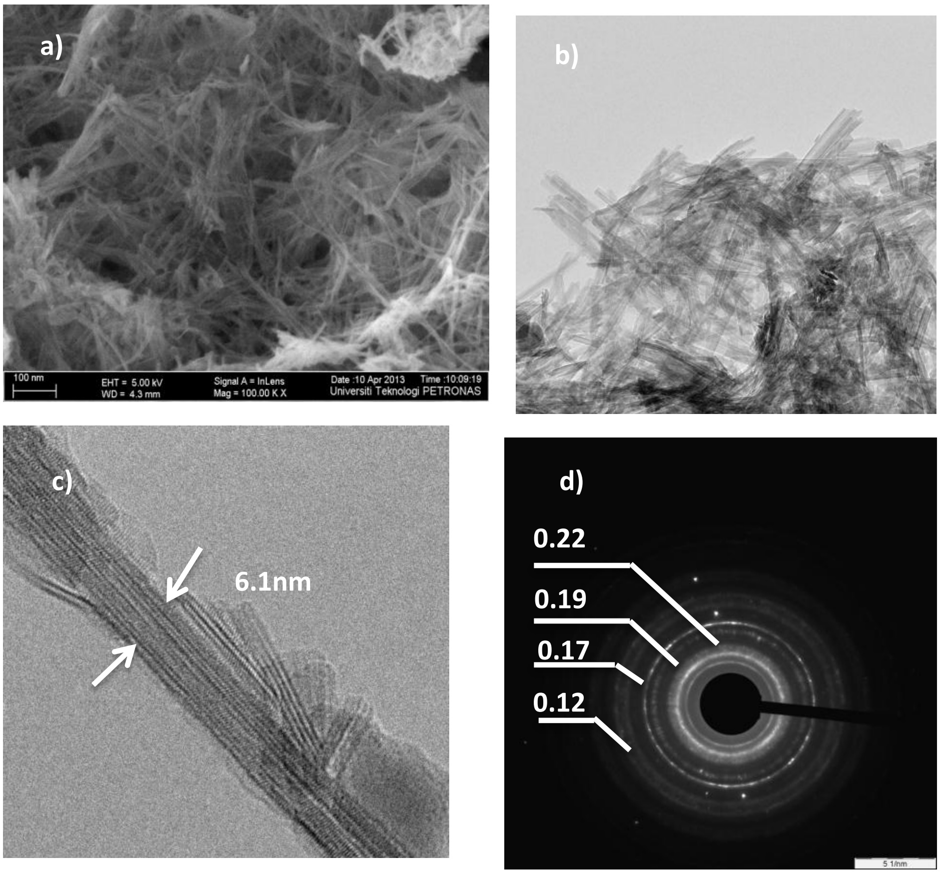

Figure 3: The FESEM image (a), TEM image (b), HRTEM image (c), and SAED (d) of TN.

Figure 3a portrays the surface morphology of the Titania nanotube from FE-SEM analysis which reveals a tube-like structure. The length of the Titania nanotubes ranges from 150-300 nm which is higher compared to the titania in Fig 2b, the TEM image reveals the titanate nanotubes at a magnification of 100nm which were formed by the pulling force from the surfactant (NaOH) while Fig 2c reveals the thickness of the tube which was measured to be 6.1 nm. Fig 3d reveals the diameters for the electron diffraction represented by (0.22, 0.19, 0.17 and 0.12 nm) from the SAED analysis. EDX analysis was done to determine the residing components in the sample, as indicated in table 3 the present components are Titanium and Oxygen with trace amount of Sodium (5.56%) because it was used as a solvent in the synthesis of the titania nanotube. The atomic concentrations (at%) of titanium and oxygen are 26.98% and 51.63%,correspondingly.

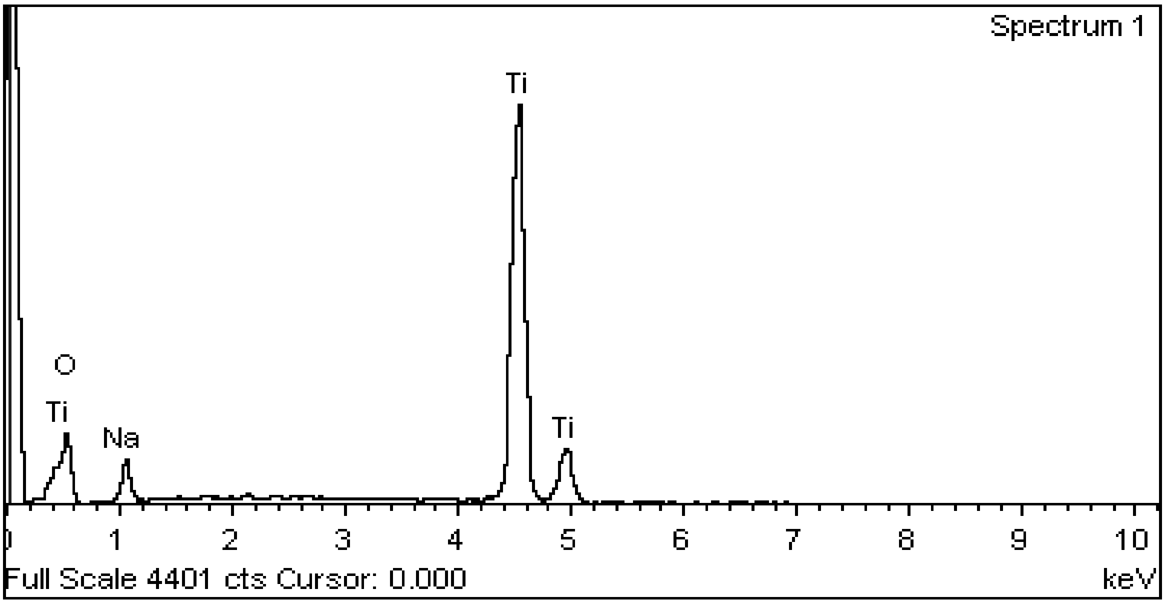

Figure 4: EDX analysis for synthesized TN

Element	**Weight %**	**Atomic %**
O K	42.81	66.97
Na K	5.56	6.05
Ti K	51.63	26.98

Table 3. EDX analysis for synthesized TN

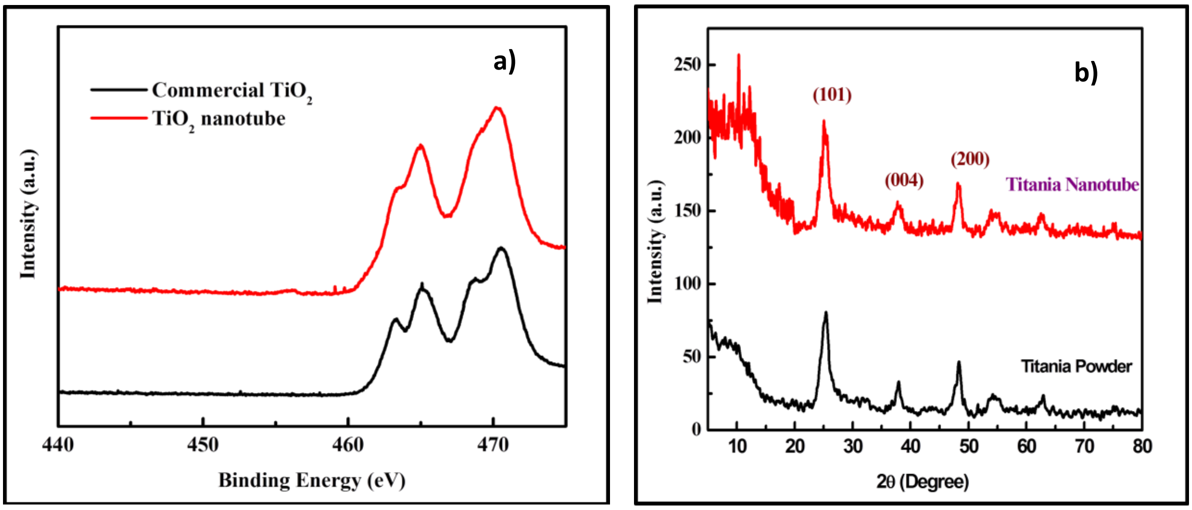

Figure 5: a) EELS analysis (b), XRD pattern for Titania and TN

The wide angle XRD pattern of commercial TiO_2 and the titanate nanotube is represented by Fig. 2b, the crystalline character is observed in the peaks. The diffraction peaks designate the formation of anatase phase, the crystal faces observed are (101), (004) and (200). Titanate nanotube is observed to be more crystalline than the titania as displayed in the XRD pattern. The Titania powder exhibits the same crystal faces at a lower intensity than the titanate nanotube [17, 18].

Figure 5a depicts the EELS for the titanate nanotube and the commercial titanium dioxide. It reveals a decrease in the binding energy of the electron state at the $2p^{3/2}$ level of titania to titanate nanotube by 465.8-464.9 eV, correspondingly. This confirms that there is a shift in the lattice planes when the commercial titania is changed to one dimensional structure (titania nanotube). The decrease in the binding energy induces a high rate of diffusion of the catalyst thus increasing its photocatalytic activity [20]. The EELS signal peak that was observed for the Ti is at 465nm which was the more prominent.

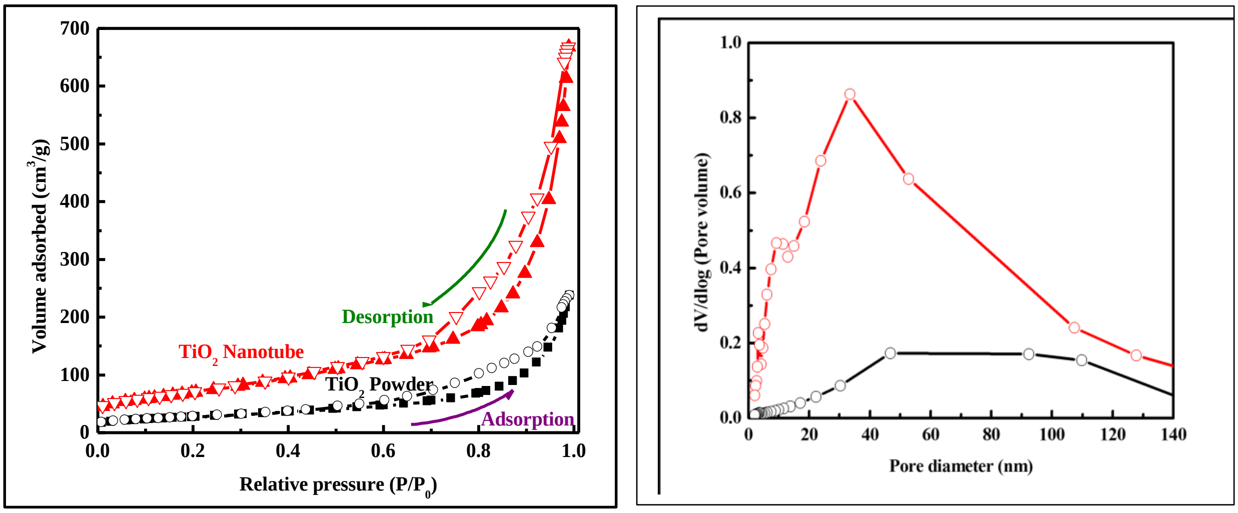

Figure 6: BET analysis (a and b) for Titania and TN

Figure 6a depicts the commercial titania and titanate nanotube adsorption and desorption Isotherms while the pore-size distribution is represented by the Barrett-Joyner-Halenda (BJH) in Fig 6b. The relative partial pressure which indicates a great change in the hysteresis loop ranges from (0.4-1.0). The behavior of the loop reveals a type v Isotherm (multilayer) which is for both Titania and titanate nanotube however the nanotube has higher adsorption area thus resulting in higher adsorption rate which makes it better than the titania [14].

A BJH analysis in Fig 6b shows that the titanate nanotube exhibits a wide pore diameter compared to the titania with a mean pore size of 20.5nm. Titania nanotube has a higher surface area and pore volume of 1.145 cm^3/g while titania is 0.738 cm^3/g. The commercial TiO_2 surface area is 244.81 m^2 /g while the titania nanotube is 277.17 m^2/g calculated by the Brunauer-Emmett-Teller (BET) method. Therefore, one-dimensional structure (titania nanotube) would prominently effective to degrade the azo dye from waste water.

4.1 WASTE WATER TREATMENT

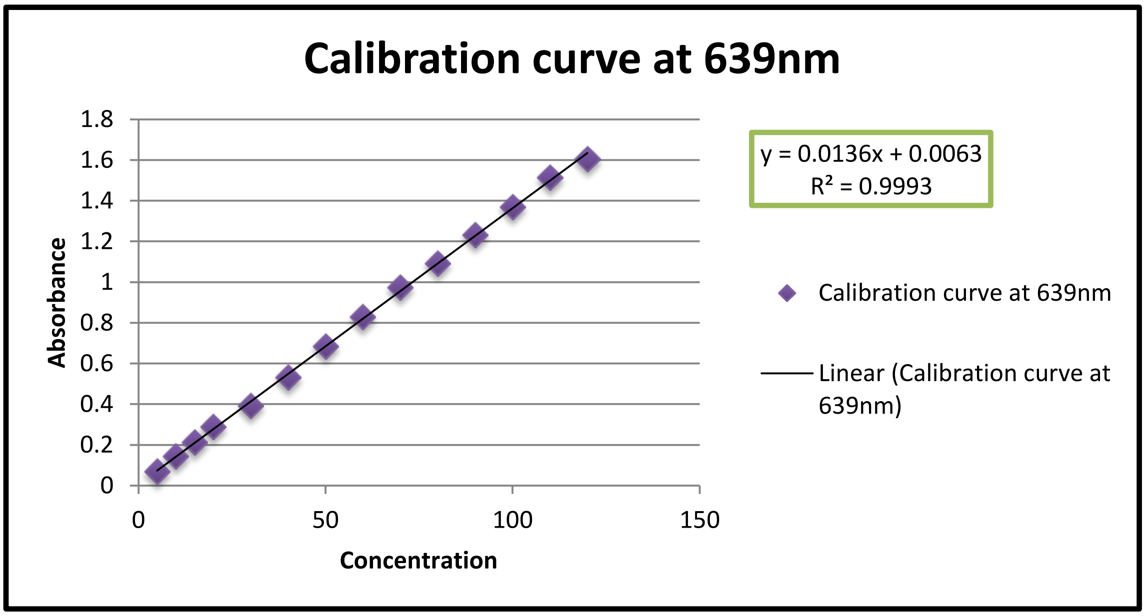

Figure 7: Calibration curve for sulfan blue dye at wavelength of 639nm with concentration of (5-120) ppm

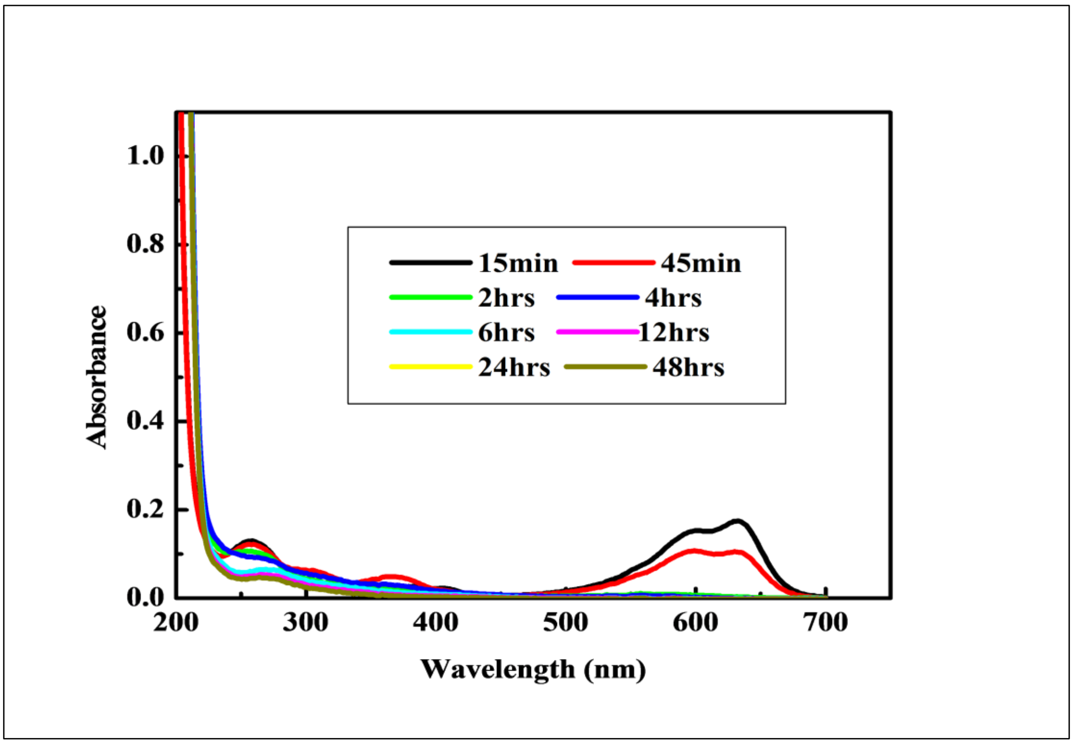

Figure 8: UV-vis changes of the SB dye in aqueous TiO_2 at different time intervals. Conditions: initial dye concentration 0.06g/L, TiO_2 0.1 g/L, and pH 8.

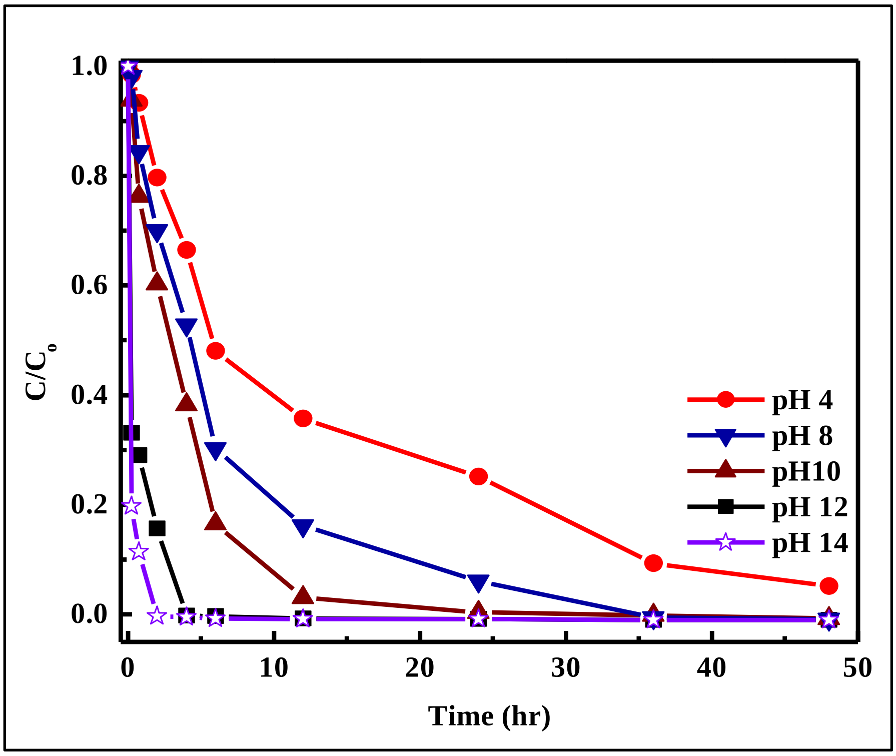

Figure 9: pH effect on the Sulfan blue degradation by commercial TiO_2. Conditions: C_o 0.06 g/L and TiO_2 0.1 g/L.

Figure 7 depicts the calibration curve which was done from a concentration range of (5-150) ppm while the degradation peak was taken at 639nm. The R^2 co-efficient is at an acceptable range of 0.9993~1 since it is in linear form. The selected wavelength range for the sulfan blue dye 200-700nm. Fig 8 portrays the UV-vis spectrum for the Sulfan blue at pH 14 which revealed a faster degradation rate. The pH was varied from acidic to base 4-14 correspondingly at duration of 48hrs. The results shown in figure 9 indicate the pH effect trend which was obtained after the degradation was done for commercial TiO_2.

Sulfan blue consist of two functional groups sulfonyl (SO^{3-}) and ethylamino group (C_2H_5-N-C_2H_5). When the pH decreases the surface is more prone to adsorption in the ethyl group. This means that the Titanium dioxide is more negative at lower pH values thus causing a higher interaction between the ethylamino group. The hydroxyl radicals formed in the valance band that degrade the Sulfan blue dye are more favourable in the ethalamino group [1]. The pH effect parameter revealed an optimum of pH 14. About 100% of the dye degrades after the 48hrs duration this was shown also in the UV-vis by the absorbance of -0.002 (a.u).

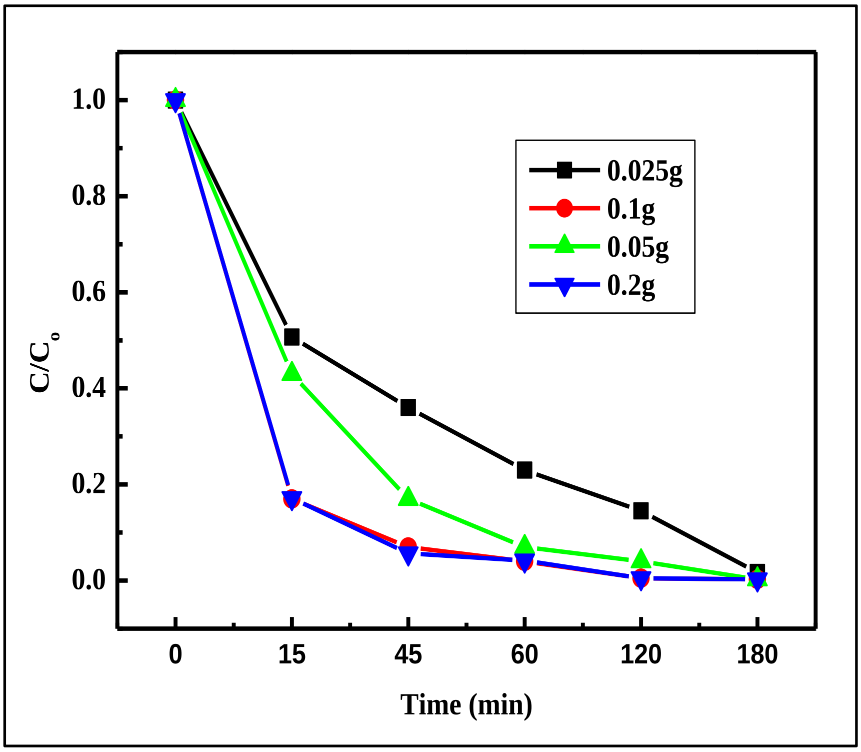

Figure 10: Dose effect on the Sulfan blue degradation by commercial TiO_2. Conditions: C_o 0.06 g/L and pH 14.

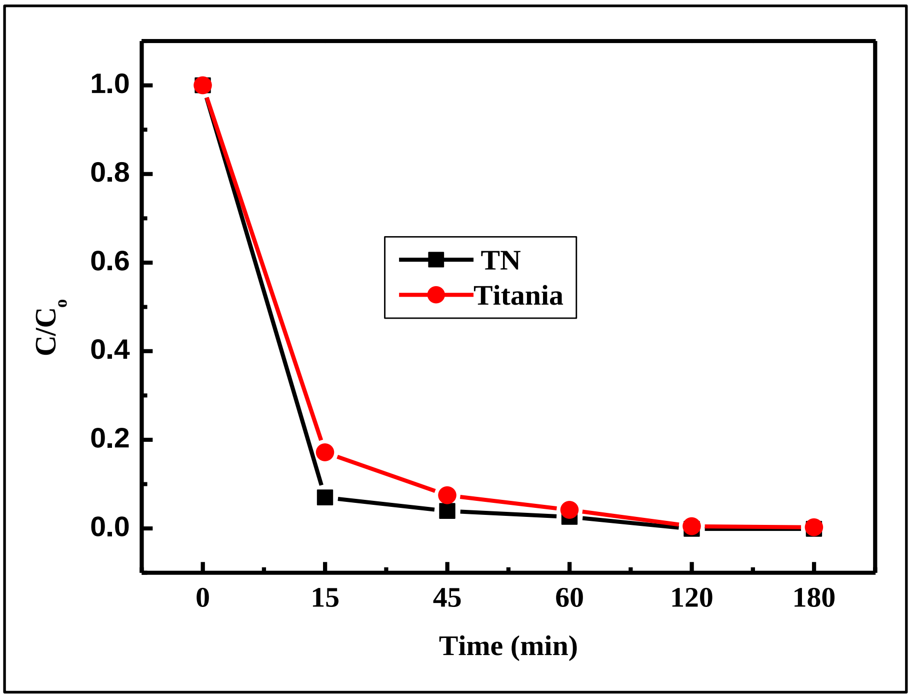

Figure 11: Comparison between Titania and TN on the Sulfan blue degradation. Conditions: C_o 0.06 g/L and pH 14 and dose 0.1 g.

Figure 10, depicts the photocatalyst dosage of commercial TiO_2 alongside the degradation rate. The dose was varied between (0.025 and 0.2) g. The results reveal that when the dose is increased the degradation is faster; from the results we can conclude that the dosage is a major parameter in the degradation of Sulfan blue dye. The increase in the degradation rate is induced by escalated contact surfaces between the dye and the titania. The practical limit in the doses was found to be at 0.2g because the results are in agreement with the one from [1]

Figure 11, compares the degradation rate of Sulfan blue with the aid of titania and titanate nanotube at a dose of 0.1g at optimum pH 14. The curve indicates that the titanate nanotube degrades the dye faster than the commercial titania. The degradation process is affected by the surface area of the photocatalyst and its crystallinity. As analyzed in the BET results the titanate nanotube exhibits a higher surface area and pore diameter, the higher surface area permits the catalyst to have more active sites thus resulting in more interactions between the dye and the photocatalyst. Moreover the higher the interaction the faster is the degradation rate.

4.2 ADSORPTION KINETICS

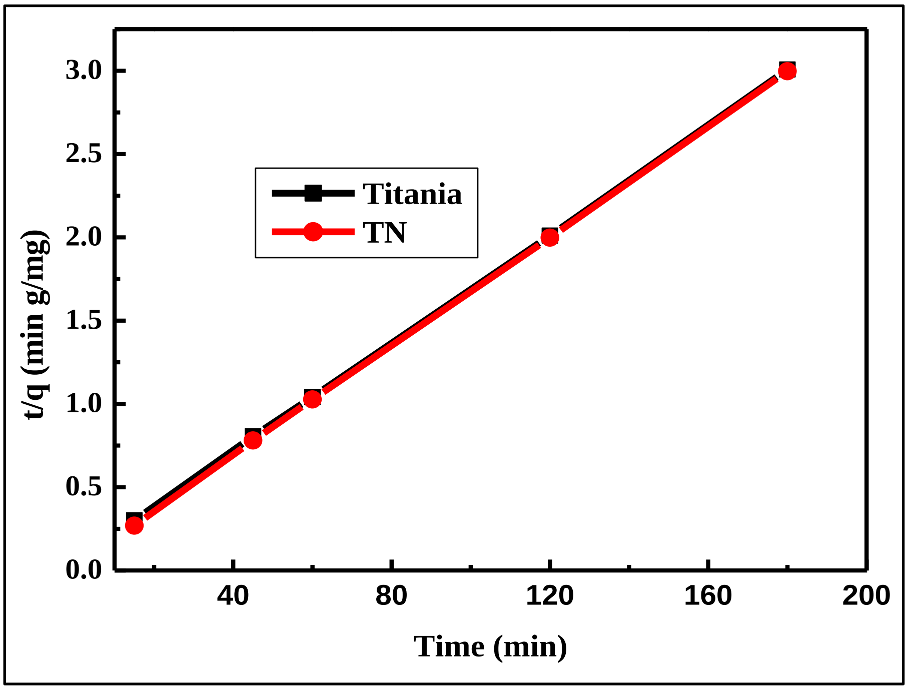

Figure 12: Type 1 Pseudo-second-order model for the adsorption of SB onto titania and TN. Conditions C_o 0.06 g/L , TiO_2 0.1 g and pH 14

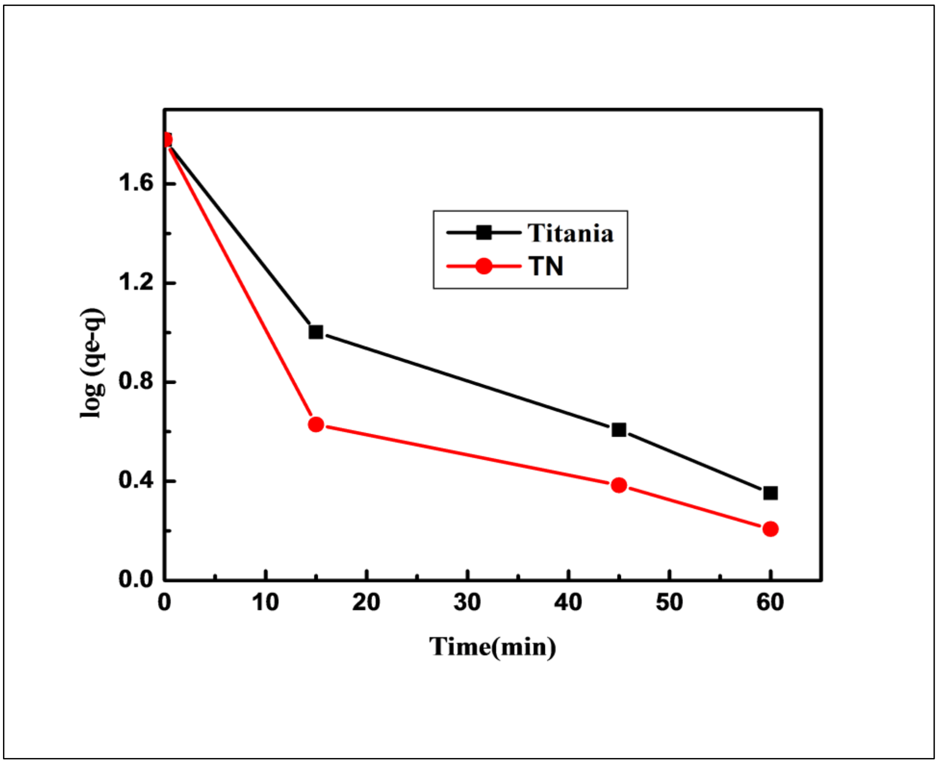

Figure 13: Type 1 Pseudo-second-order model for the adsorption of SB onto titania and TN. Conditions C_o 0.06g/L , TiO_2 0.1 g and pH 14

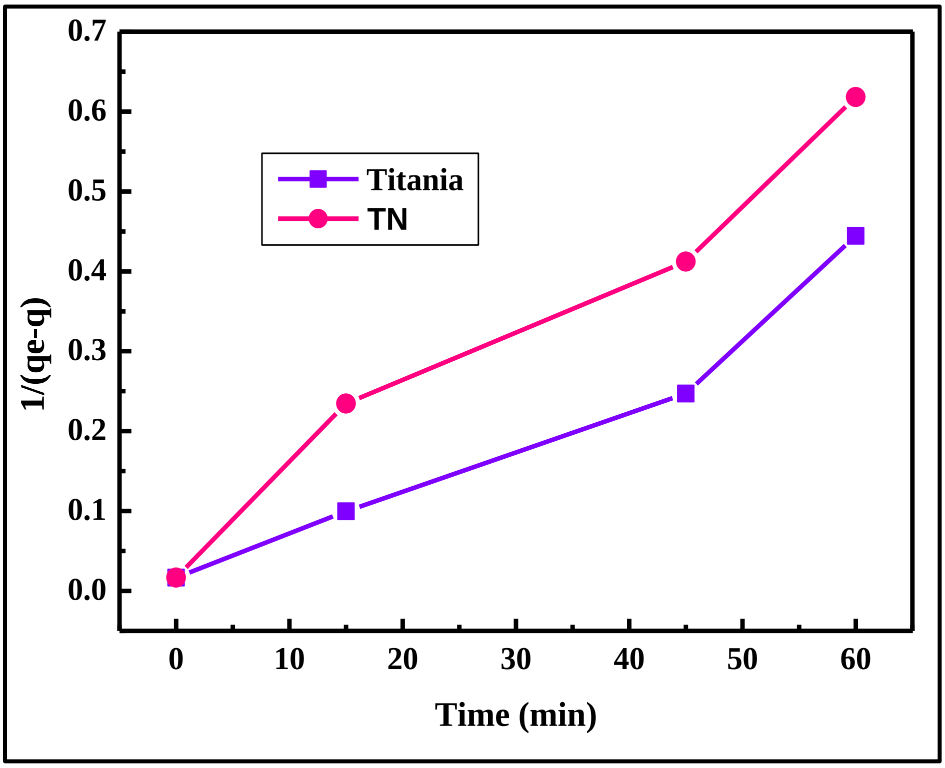

Figure 14: Type 5 Pseudo-second-order model for the adsorption of SB onto titania and TN. Conditions C_o 0.06g/L , TiO_2 0.1 g and pH 14.

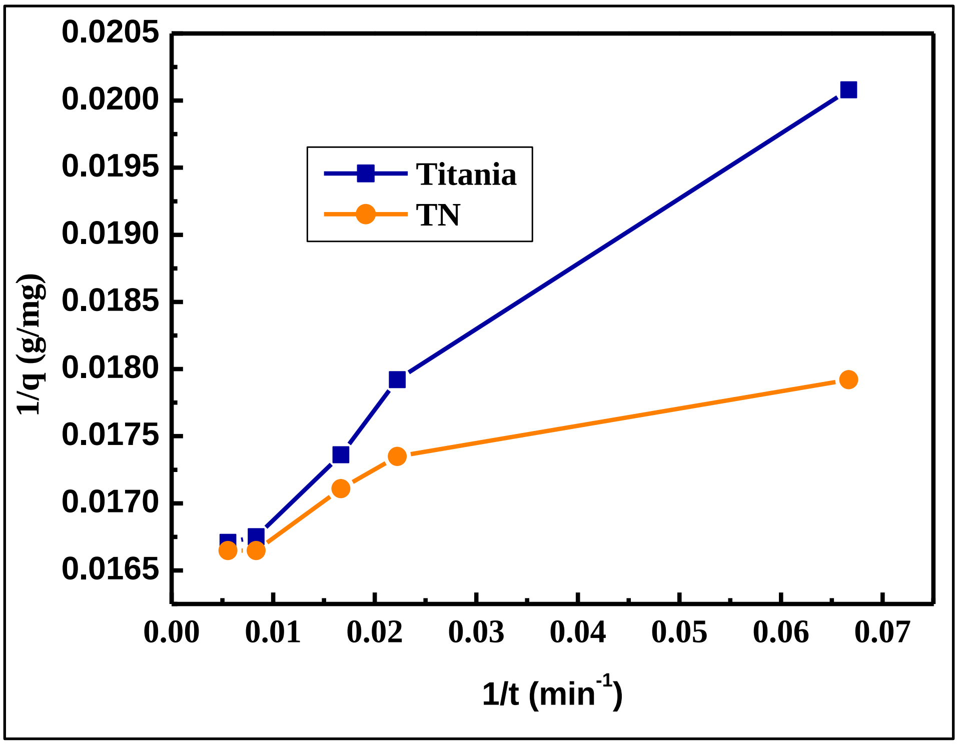

Figure 15: Type 2 Pseudo-second-order model for the adsorption of SB onto titania and TN. Conditions C_o 0.06g/L , TiO_2 0.1 g and pH 14.

Kinetic models were analyzed upon the comparison of titania and titanate nanotube. The initial concentration was kept constant at 60ppm with pH 14 and photo catalyst dose of 0.1g. The data from Fig 12 was fitted in a Type 1 pseudo second order model represented by the equation (1):

$$\frac{t}{q} = \frac{1}{K_s qe^2} + \frac{1}{qe} t \qquad (1)$$

Where, q_e is the amount of Sulfan blue adsorbed per mass of adsorbent (mg/g) at equilibrium, K_s is the Pseudo-second order equation [g/mg min] and t is time (min). Table 1 shows the constants that are depicted from the graph. Fig 13 shows the fit of the pseudo-first-order model which is governed by the equation (2). The constants are Obtained from the plot of log (qe-q) versus t.

$$\log(qe - q) = \log qe - \frac{K_1 t}{2.303} \qquad (2)$$

Where, K_1 is the adsorption rate, q is the amount of dye adsorbed (mg/g). The constants are represented by table 4. The degradation data was also fitted in the Type 2 pseudo-second-order model with the equation:

$$\frac{1}{q} = \left(\frac{1}{K_2 qe^2}\right)\frac{1}{t} + \frac{1}{qe} \qquad (3)$$

Fig. 14 portrays the type 5 pseudo second-order model which is represented by equation 4 while the adsorption constants following this model are also represented in table 4.

$$\frac{1}{qe - q} = \left(\frac{1}{qe}\right) + K_2 t \qquad (4)$$

From the results represented by table 4, the best fit with the highest coefficient is the type 1 pseudo second order model.

	Pseudo-first-order				**Type 1 Pseudo second order**			**Type 2 Pseudo second order**			**Type 5 Pseudo second-order**		
pH 14	$q_{e,exp}$ (mg/g)	q e	K_1	R^2	q_e,cal	K_2	R^2	q_e,cal	K_2	R^2	qe,cal	K^2	R^2
TN	60.066	26.8	0.05	0.76	60.6	0.0087	1	49.26	0.013	0.889	769	0.007	0.95
Titania	59.85	38.3	0.05	0.97	57.1	-0.003	1	17.986	0.005	0.988	22.6	0.009	0.97

Table 4: Pseudo-first-order, type 1, type 2 and type 5 pseudo-second-order model parameters for Titania and TN comparison.

The table shown above represents the kinetic models as shown in Fig. (12-15). The type 1 pseudo second-order model proved to be the best fit for the experimental data with an R^2 value that is greater than 0.99 for both the titanate nanotube and titania.in addition the pseudo-second order foresees rational qe values. The lower value of R^2 is found in the Pseudo first order that suggest that the kinetic model is not fit for the experimental data, however the coefficient is only lower for the titanate nanotube and higher for titania as seen in table1 moreover the model failed to predict the practical qe values.

The same trend is observed in the type 5 pseudo-second order model, the R^2 values are reasonable however the qe values are out of range thus it is inappropriate to use the type 5 pseudo second-order model. Linear models simulates that the points follow the Gaussian distribution, this assumption hardly ever true when converting the experimental data [11]. With the pH kept at a constant rate, the difference in the surface morphology that was studied earlier results in the difference in the R values. The table suggests that if the surface area of the titania is increased even further to the two and three dimensional structure the kinetic data will be along the pseudo-second order model because between the titania and nanotube there is an increase in the R^2 value and also accurate results for the qe are observed.

CHAPTER 5

CONCLUSION

The one dimensional structure (titanate nanotube) was synthesized through the hydrothermal route. The results have been displayed using the characterization such as the FESEM and HRTEM to verify the presence of the nanotubes in the sample. The degradation results were based on evaluating the effect of increasing dosage and varying the pH of the dye solution. The results show that when the pH is increased (alkaline) there is a higher rate in the degradation. An optimum pH was obtained (pH 14) and from the pH effect analysis the dosage effect was done. The dose effect results reveal that as the photocatalyst dosage is increased so does the rate of degradation. Moreover the degradation was done with the Titanate nanotube which shows a faster rate of degradation than the commercial TiO_2.The kinetic data indicate that the degradation of Sulfan blue is a Type 1 Pseudo-second-order model. The study can be furthered by studying the regeneration process of the TiO_2 as well as the binary dye degradation. This study can be implemented in a large scale to alleviate the problem faced in industries today of dyes leaking into waste water however more studies can be conducted to assess the regeneration cycle of the photocatalyst. There are numerous parameters that affect the rate of degradation moreover if they are carefully analyzed the dye will be degraded effectively and efficiently.

REFERENCES

1. Chen, C.C., et al., *Photooxidative N-de-ethylation of anionic triarylmethane dye (sulfan blue) in titanium dioxide dispersions under UV irradiation.* Journal of Hazardous materials, 2006. 137(3): p. 1600─1607.
2. Ji, P., et al., *Study of adsorption and degradation of acid orange 7 on the surface of CeO_2 under visible light irradiation.* Applied Catalysis B: Environmental, 2009. 85(3–4): p. 148─154.
3. Juang, R.-S., S.-H. Lin, and P.-Y. Hsueh, *Removal of binary azo dyes from water by UV-irradiated degradation in TiO_2 suspensions.* Journal of Hazardous materials, 2010. 182(1–3): p. 820─826.
4. Kapinus, E.I. and T.I. Viktorova, *Kinetics of the photocatalytic degradation of methylene blue on titanium dioxide.* Theoretical and Experimental Chemistry, 2010. 46(3): p. 163─167.
5. Madhusudan Reddy, K., S.V. Manorama, and A. Ramachandra Reddy, *Bandgap studies on anatase titanium dioxide nanoparticles.* Materials chemistry and physics, 2003. 78(1): p. 239─245.
6. Khataee, A.R. and M.B. Kasiri, *Photocatalytic degradation of organic dyes in the presence of nanostructured titanium dioxide: Influence of the chemical structure of dyes.* Journal of Molecular Catalysis A: Chemical, 2010. 328(1–2): p. 8─26.
7. Mukhlish, M.Z., et al., *Papaya (Carica papaya L.) Leaf Powder: Novel Adsorbent for Removal of Methylene Blue from Aqueous Solution.* Water, Air, & Soil Pollution, 2012. 223(8): p. 4949─4958.
8. Sauer, T., et al., *Kinetics of photocatalytic degradation of reactive dyes in a TiO_2 slurry reactor.* Journal of Photochemistry and Photobiology A: Chemistry, 2002. 149(1–3): p. 147─154.
9. Nguyen-Phan, T.-D. and E.W. Shin, *Morphological effect of TiO_2 catalysts on photocatalytic degradation of methylene blue.* Journal of industrial and engineering Chemistry, 2011. 17(3): p. 397─ 400.
10. Subramani, A.K., et al., *Photocatalytic degradation of indigo carmine dye using TiO_2 impregnated activated carbon.* Bulletin of Materials Science, 2007. 30(1): p. 37─ 41.

11. Kumar, K.V., *Linear and non-linear regression analysis for the sorption kinetics of methylene blue onto activated carbon.* Journal of Hazardous materials, 2006. 137(3): p. 1538— 1544.

12. Ding, X., et al., *Synthesis of square-like anatase* TiO_2 *nanocrystals based on* $TiOF_2$ *quantum dots.* Journal of Alloys and Compounds, 2013. 550(0): p. 475— 478.

13. Archana, J., M. Navaneethan, and Y. Hayakawa, *Hydrothermal growth of monodispersed rutile* TiO_2 *nanorods and functional properties.* materials letters, 2013. 98(0): p. 38— 41.

14. Hung, I.M., et al., *Preparation and characterization of mesoporous* TiO_2 *thin film.* Journal of Porous Materials, 2010. 17(4): p. 509— 513.

15. Nguyen-Phan, T.-D., et al., *Synthesis of hierarchical rose bridal bouquet- and humming-top-like* TiO_2 *nanostructures and their shape-dependent degradation efficiency of dye.* Journal of Colloid and Interface Science, 2011. 356(1): p. 138— 144.

16. Thennarasu, G., A. Sivasamy, and S. Kavithaa, *Synthesis, characterization and catalytic activity of nano size semiconductor metal oxide in a visible light batch slurry photoreactor.* Journal of molecular Liquids, 2013. 179(0): p. 18— 26.

17. Wei, J., et al., *Hydrothermal growth of titania nanostructures with tunable phase and shape.* materials letters, 2007. 61(23–24): p. 4610— 4613.

18. Xiang, Q. and J. Yu, *Photocatalytic Activity of Hierarchical Flower-Like* TiO_2 *Superstructures with Dominant {001} Facets.* Chinese journal of catalysis, 2011. 32(3–4): p. 525— 531.

19. Li, Z., et al., *Facile preparation of squarylium dye sensitized* TiO_2 *nanoparticles and their enhanced visible-light photocatalytic activity.* Journal of Alloys and Compounds, 2013. 564(0): p. 138— 142.

20. Li, P., et al., *In situ preparation of Ni–Cu/*TiO_2 *bimetallic catalysts.* Journal of Catalysis, 2009. 262(1): p. 73— 82.

APPENDIX

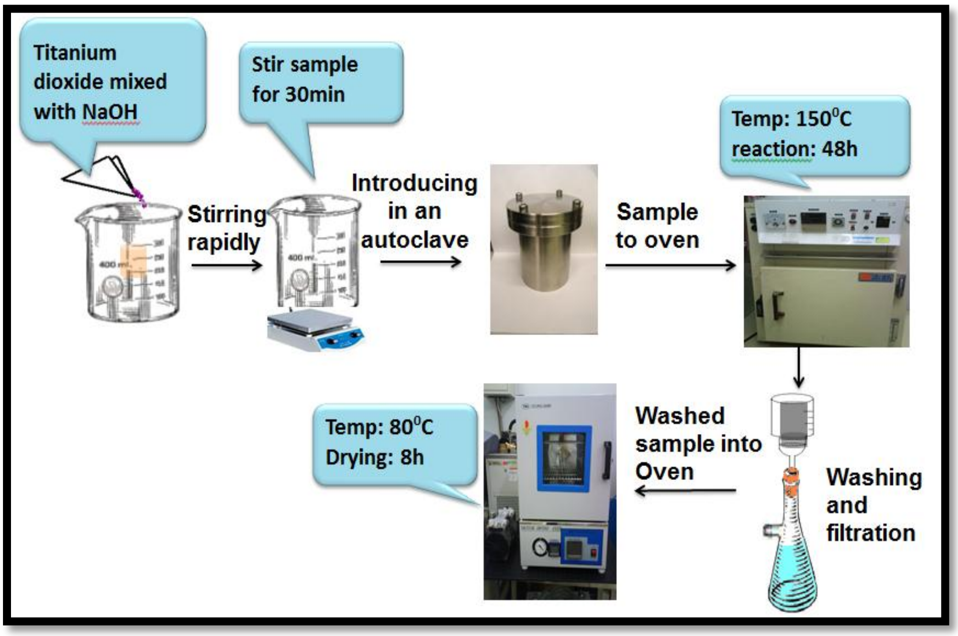

Figure 16: Procedure for the synthesis of TN through the hydrothermal route

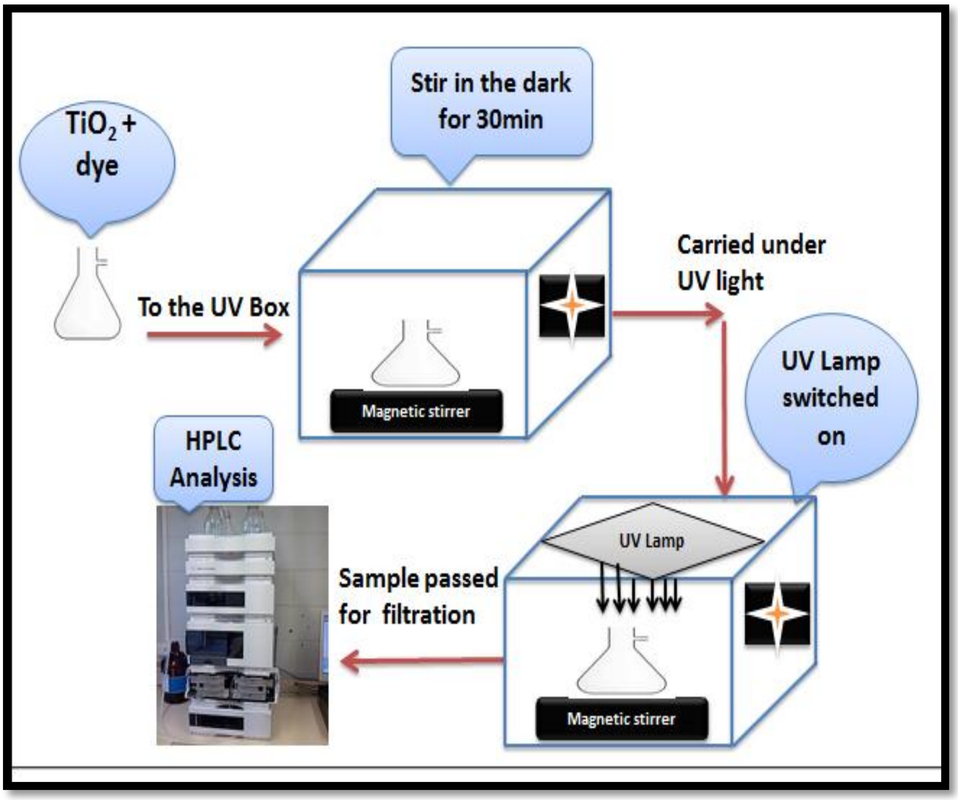

Figure 17: Procedure for the degradation of Sulfan blue dye through photocatalysis process

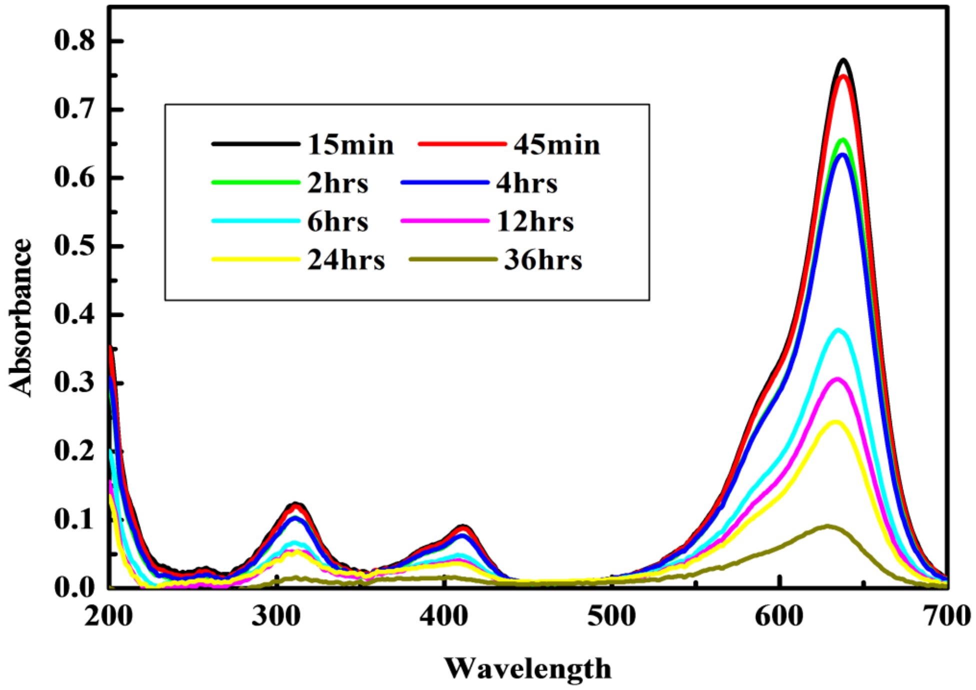

Figure 18: UV-vis changes of the SB dye in aqueous TiO_2 at different time intervals. Conditions: initial dye concentration 0.06 g/L, TiO_2 0.1 g/L, and pH 4.

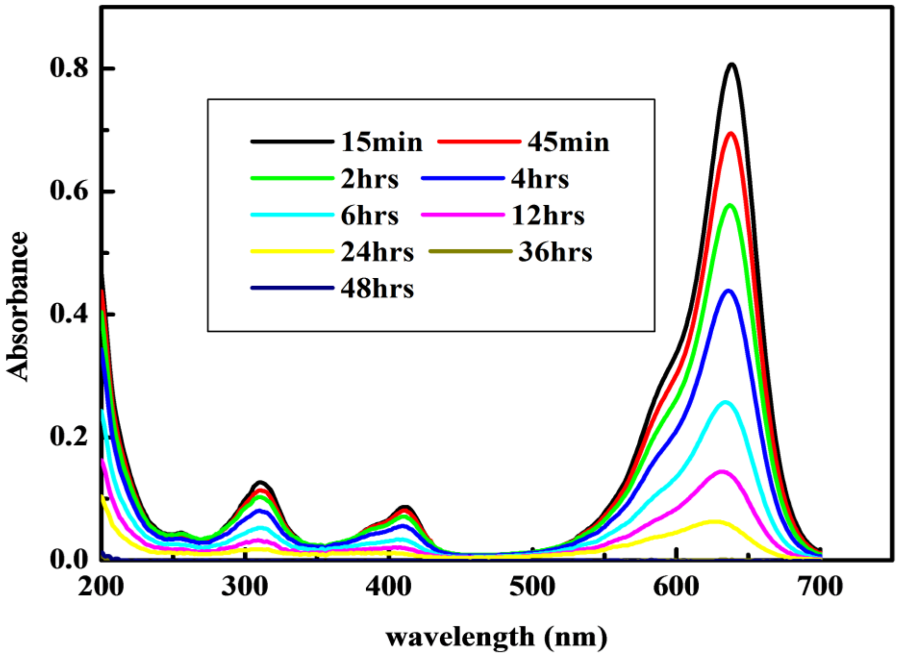

Figure 19: UV-vis changes of the SB dye in aqueous TiO_2 at different time intervals. Conditions: initial dye concentration 0.06g/L, TiO_2 0.1 g/L, and pH 8.

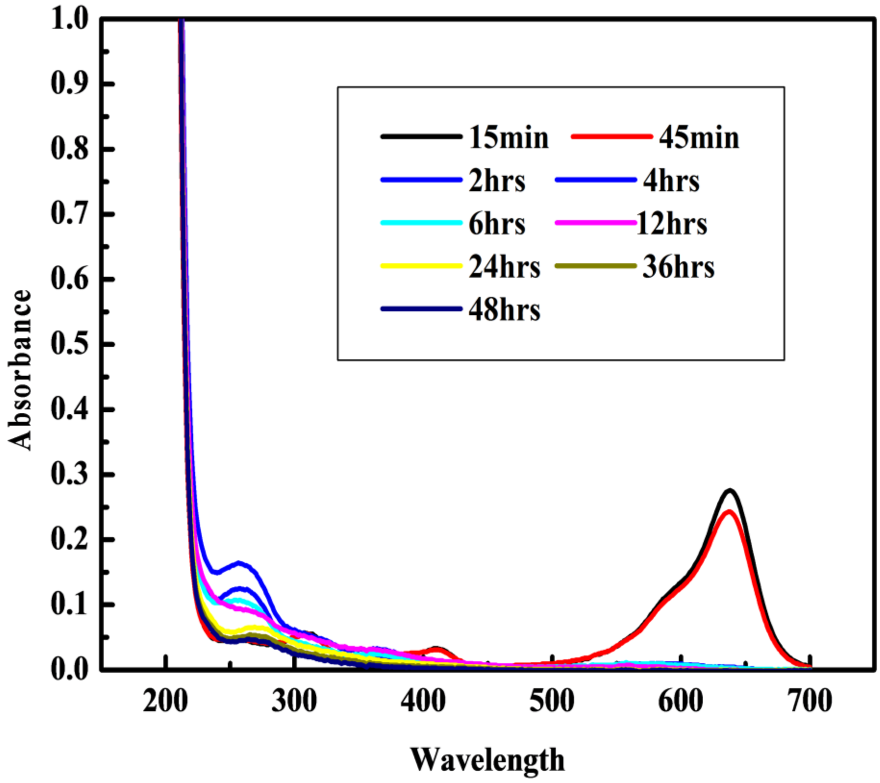

Figure 21: UV-vis changes of the SB dye in aqueous TiO_2 as a function of time. Conditions: initial dye concentration 0.06g/L, TiO_2 0.1g/L, and pH 12.

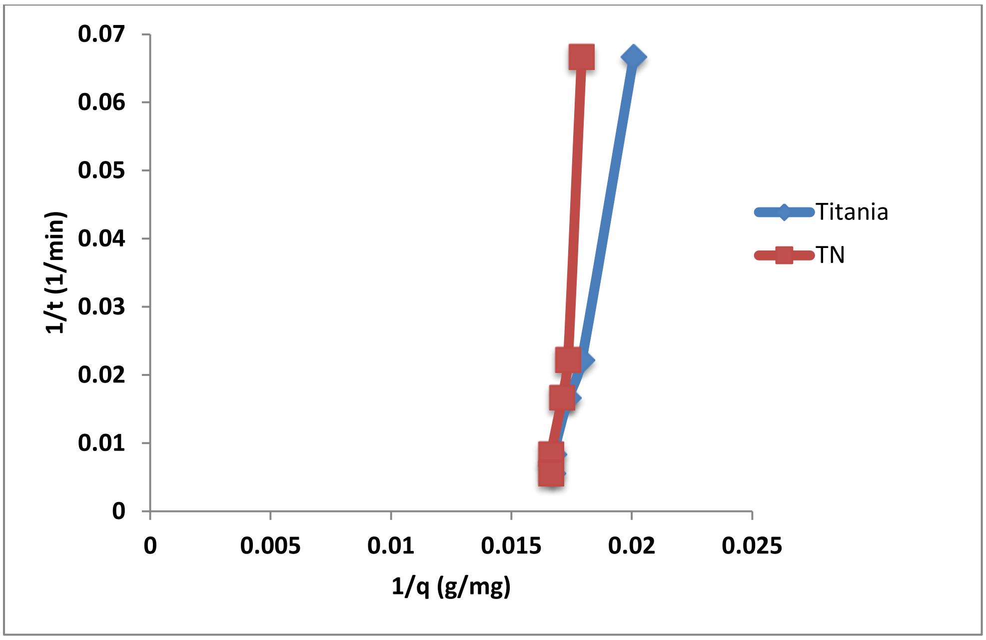

Figure 22: Type 3 Pseudo-second-order model for the adsorption of SB onto titania and TN. Conditions C_o 0.06 g/L , TiO_2 0.1g and pH 14.

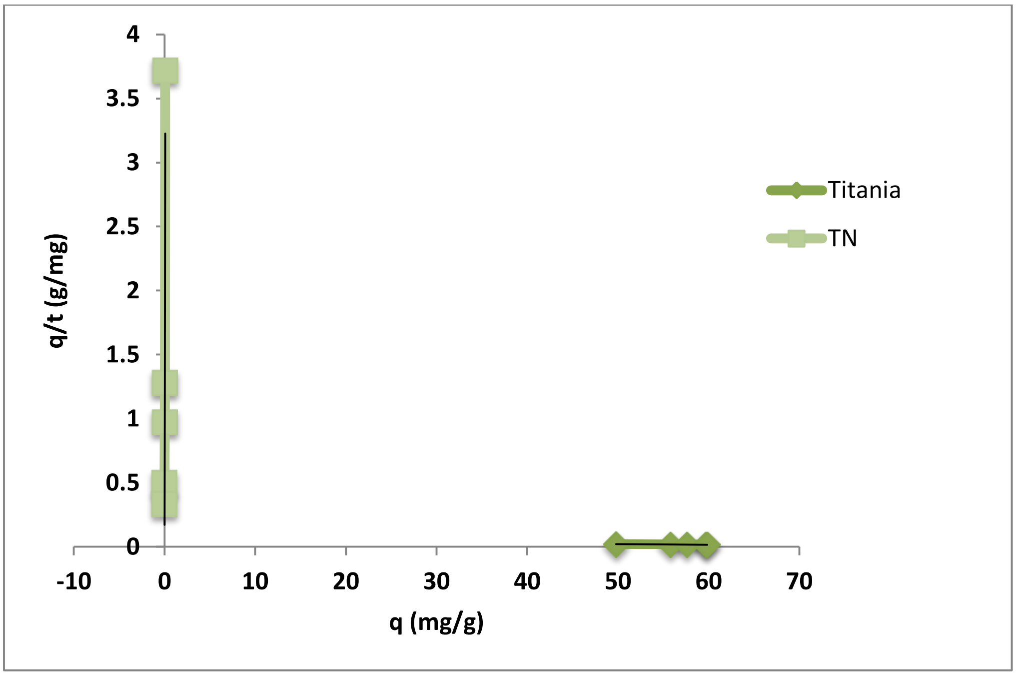

Figure 23: Type 4 Pseudo-second-order model for the adsorption of SB onto titania and TN. Conditions C_o 0.06 g/L , TiO_2 0.1 g and pH 14.

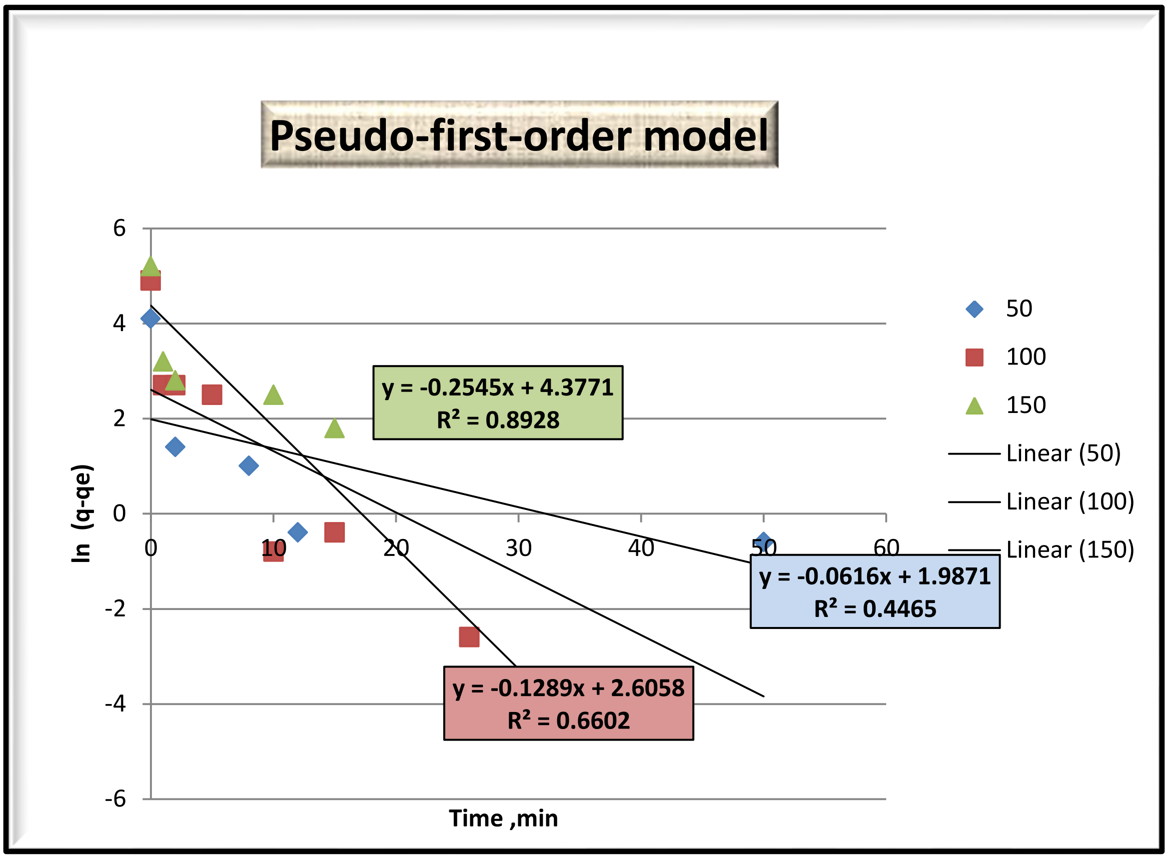

Figure 24: Pseudo-first-order model for the adsorption of Methylene blue onto PLP. Conditions: C_o 50,100,150 mg/L, volume 0.2 L, weight 0.1g.

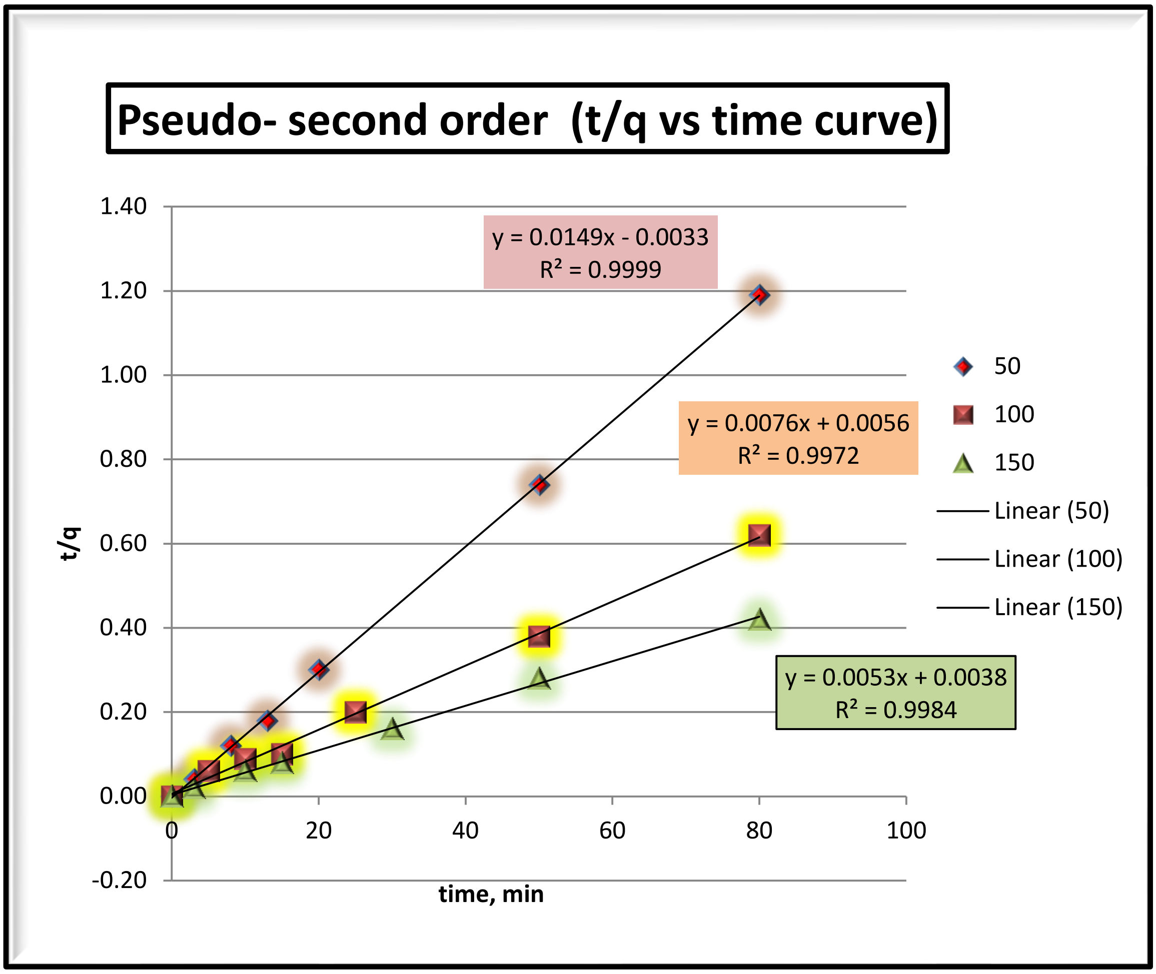

Figure 25: Pseudo-second-order model for the adsorption of Methylene blue onto papaya leaf. Conditions: C_o 50,100,150 mg/L , volume 0.2 L, weight 0.1g.

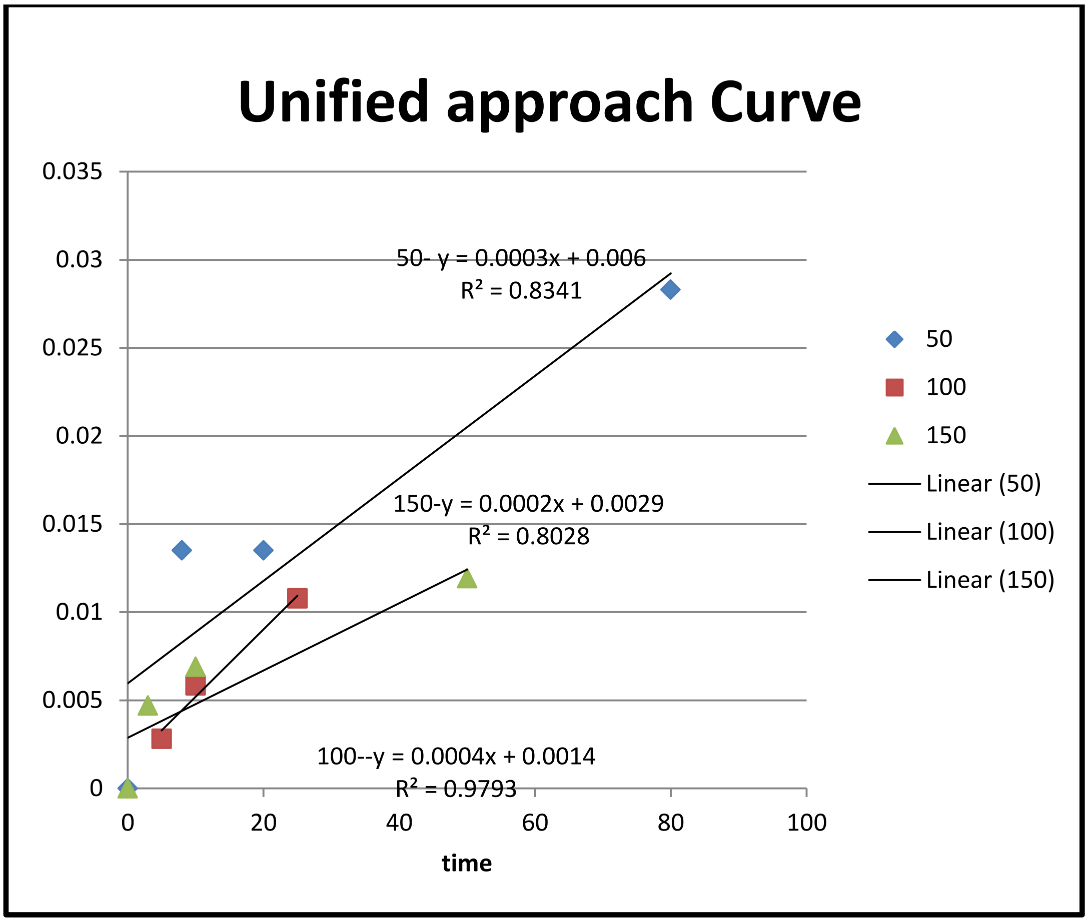

Figure 26: Unified Model approach for the adsorption of Methylene blue onto papaya leaf. Conditions: C_o 50,100,150 mg/L , volume 0.2 L, weight 0.1 g.

	Pseudo-first-order				**Pseudo second order**			**Unified approach Model**		
Initial concentration (c_o,mg/L)	$q_{e,exp}$ (mg/g)	q e	K_{ad}	R^2	q_e,cal	K_2	R^2	q_e,cal	K_2	R^2
50	68.12	7.3	0.06	0.45	67.11	0.07	1.00	67.23	0.003	0.3
100	128.14	9.6	0.13	0.66	131.58	0.01	1.00	127.86		
150	179.44	79.6	0.25	0.89	188.68	0.007	1.00	181.25		

Table 5: Pseudo-first-order, pseudo-second-order, and unified approach kinetic model parameters at various initial concentration of the methylene blue dye

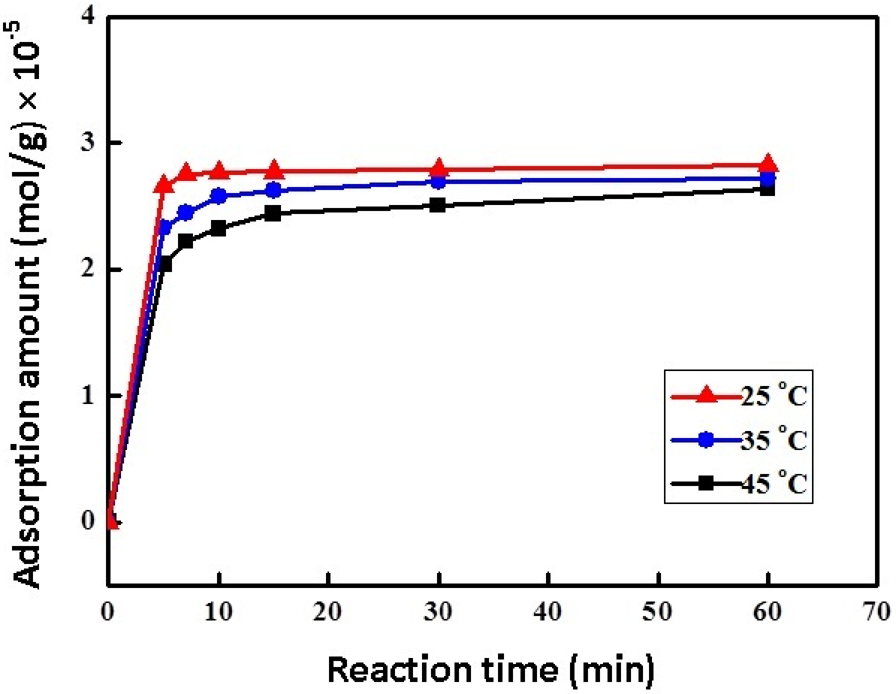

Figure 27: Adsorption isotherms of perchloroethylene onto TNs at different temperatures and constant pH 4.

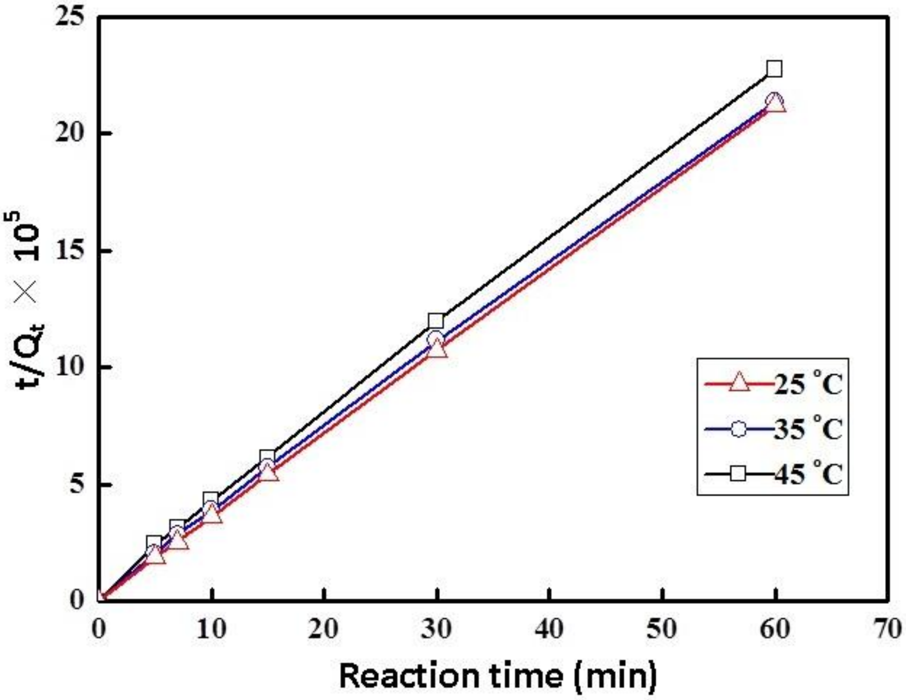

Figure 28: Kinetic model of pseudo-second order reaction for perchloroethylene adsorption onto TN. Conditions: initial perchloroethylene concentration 900 mg/L and pH 4.

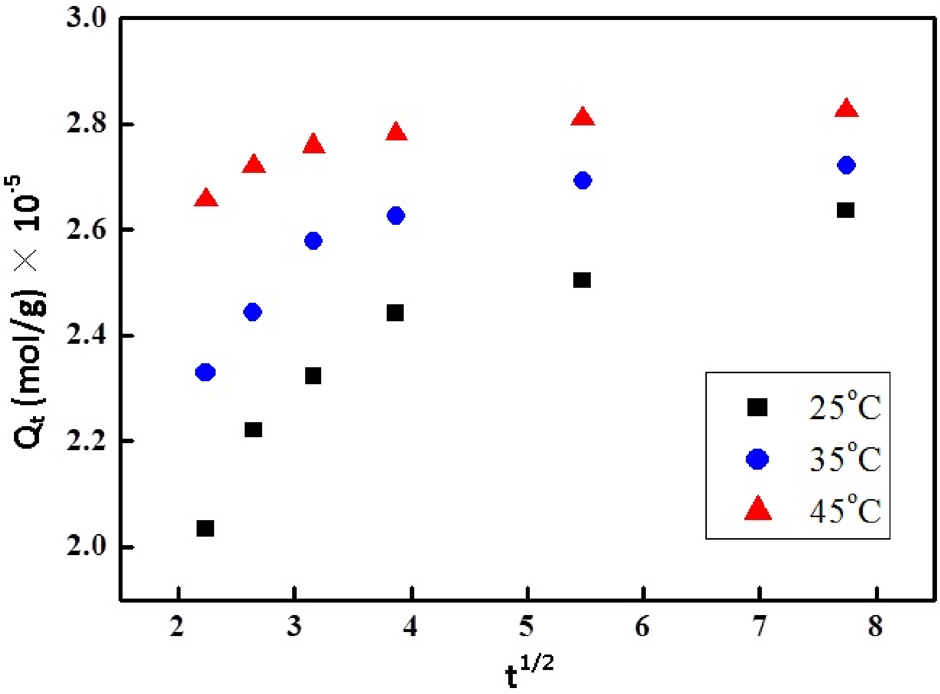

Figure 29: The diffusion model plots for the adsorption of perchloroethylene onto TN. Conditions: initial perchloroethylene concentration 900 mg/L, 25, 35 and 45 °C, and pH 4.

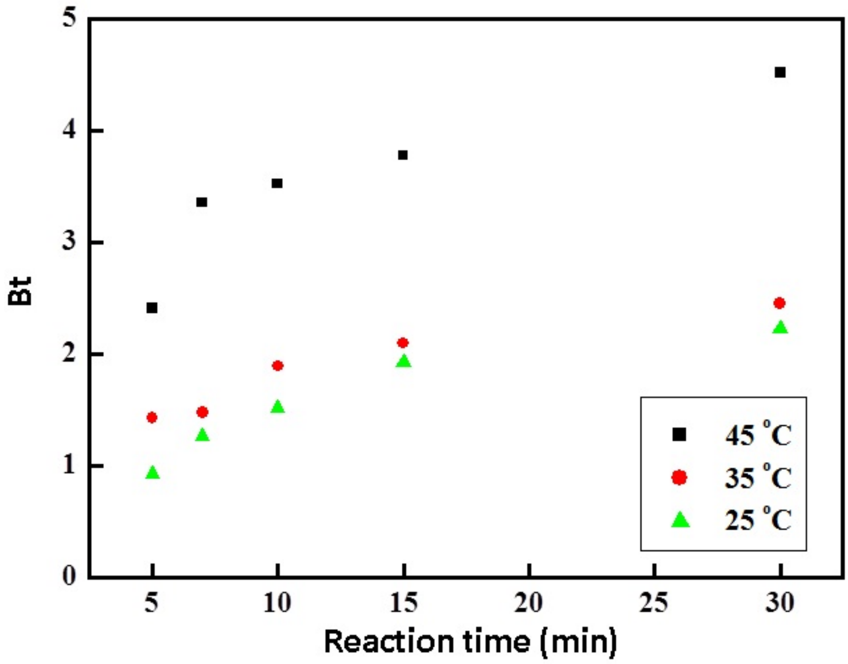

Figure 30: Correlation between Bt and t for perchloroethylene adsorption onto TN. Conditions: initial perchloroethylene concentration 900 mg/L, 25, 35 and 45 °C, and pH 4

T(^oC)	**Q_m**	**β**	**E**
	(mol/g)x 10^{-3}	**(mol^2/J^2)x10^{-9}**	**(kJ/mol)**
25	123	-6.01	-9.13
35	131	-7.02	-8.43
45	164	-8.19	-7.82

Table 6: The initial concentration and condition of perchloroethylene solution were 900mg/L and pH= 4, respectively.

T(^oC)	**Pseudo second-order model**		
	K (g/mol min) x 10^4	**Q_e (mol/g) x 10^{-3}**	**R^2**
25	16.2	2.81	0.999
35	3.01	2.84	0.999
45	2.23	2.68	0.999

Table 7: The initial concentration and condition of perchloroethylene solution were 900mg/L and pH=4, respectively.